Journal of Luminescence 134 (2013) 678–685

Contents lists available at SciVerse ScienceDirect

Journal of Luminescence

journal homepage: www.elsevier.com/locate/jlumin

Effect of pressure on the free ion and crystal field parameters of Sm^{2+} in BaFBr and SrFBr hosts

Prodipta Pal*, Tiphaine Penhouët, Vincenza D'Anna, Hans Hagemann

Département de Chimie Physique, Sciences II, Université de Genève 30, Quai Ernest-Ansermet, CH-1211 Genève 4, Switzerland

ARTICLE INFO

Article history:
Received 30 March 2012
Received in revised form
10 July 2012
Accepted 16 July 2012
Available online 7 August 2012

Keywords:
Sm^{2+}
High pressure luminescence
Crystal field
BaFBr
SrFBr

ABSTRACT

The emission spectra of Sm^{2+} doped in BaFBr and SrFBr hosts were measured at 10 K from ambient pressure to 8 GPa. The crystal field energy levels determined from the emission spectra were used to extract the free ion parameters (F_k and ζ) and crystal field parameters (B_q^k). The variation of F_k and ζ as a function of pressure was studied systematically and was discussed in relation to the central field and symmetry restricted covalency models. The change of the spin–orbit coupling parameter (ζ) with pressure for SrFBr:Sm^{2+} showed very different behavior than in other matlockite hosts. Moreover the variation of B_q^k under pressure was studied. The pressure dependence of the B_q^k was described quantitatively using the Superposition Model (SM) with the help of structural parameters as a function of pressure, obtained from periodic DFT calculations. The validity of the SM was tested for Sm^{2+} in BaFBr and SrFBr. It is shown that this model does not apply to SrFBr, in contrast to other matlockite host materials.

1. Introduction

The interactions of the lanthanide ions with their surroundings are commonly described using crystal field models, in particular the superposition model (SM) [1]. The observation that crystal field parameters of trivalent $4f^n$ ions are quite similar to those of $4f^{n\pm1}$ ions in the same host (e.g., Ln^{3+}:$LaCl_3$ [2]) strongly supports this approach.

Studies of crystal field parameters of divalent rare earth ions in crystals are not very frequent [3]. Eu^{2+}-doped crystals find many applications such as blue phosphor, X-ray detectors or in the persistent phosphor $SrAl_2O_4$:Eu^{2+}, Dy^{2+}. The optical study of Sm^{2+}, which can present many *f–f* transitions, is thus expected to give additional informations about the crystal field experienced by Eu^{2+} in the same host.

Sm^{2+}-doped crystals have many interesting properties such as room temperature hole burning [4] and potential pressure sensors [5]. Sm^{3+}-doped BaFCl nanocrystals have recently been shown to present efficient X-ray storage properties [6–8]. The storage mechanism is based on the reduction of Sm^{3+} to Sm^{2+} upon ionization radiation [7]. Sm^{2+} can be bleached optically back to Sm^{3+}. Both X-ray induced reduction and photobleaching can be modeled assuming dispersive first-order kinetics [7]. Recently, photoluminescence of Sm^{2+}/Sm^{3+} doped in $Sr_4Al_{14}O_{25}$ was studied [9], also the luminescence of Sm^{2+} was used to monitor pressure induced phase transitions in $BaBr_2$ [10].

Crystals within the Matlockite (PbFCl-structure) family MFX (with M=Ca, Sr, Ba and X=Cl, Br, I) are an interesting subject of investigation for various reasons. Luminescence from BaFI and $BaFBr_{1-x}I_x$ crystals originates from self-trapped exitons [11]. Matlockites are useful for commercial applications (Eu-doped BaFBr in imaging plates [12]). They form solid solutions such as $SrFCl_xBr_{1-x}$ [13] which lead to an important inhomogeneous broadening of the Sm^{2+} emission [4,14], a condition for optical hole burning at high temperature. The relatively high symmetry (the site symmetry of the metal ion is C_{4v}) allows to distinguish with relatively few parameters cubic and axial contributions to the crystal field. EPR measurements on S-state ions, in particular Eu^{2+}, in MFX crystals showed a linear correlation of the b_2° crystal field parameter (indicative of an axial contribution) with the '*a*' lattice parameter [15].

The shielding of the 4f electrons by the 5p and 6s electrons leads to a small crystal field created by the surrounding ligands. This causes relatively small shifts and splittings of the free ion levels. For that reason, lanthanide ions are good probes to study the crystal-field effect. With the application of high pressure, the interatomic distances change continuously and therefore the crystal field can be modulated without perturbing other physical properties like the point symmetry of the lanthanide ion site or the chemical composition of the samples. The change of the free ion and crystal field parameters under high pressure of Sm^{2+} in MFCl (M=Ca, Sr, Ba) has been studied previously in detail (e.g.,

* Corresponding author. Tel.: +41223796106; fax: +41223796103.
E-mail address: prodipta.pal@unige.ch (P. Pal).

0022-2313/$ - see front matter © 2012 Elsevier B.V. All rights reserved.
http://dx.doi.org/10.1016/j.jlumin.2012.07.010

[16], [17]). Pressure dependent emission spectra of Sm^{2+} in SrFBr, BaFBr and BaFI showed quasi linear shifts of the ^5D_J—^7F_J emission bands [18,19].

In this paper we study the dependence on pressure of the free ion parameter and crystal field parameters of Sm^{2+} ion in BaFBr and SrFBr and address the validity of the superposition model in these compounds.

2. Experimental

Crystalline samples were obtained by slow cooling of stoichiometric melts of the constituent halides (e.g., SrF_2+SrBr_2) under inert or hydrogen atmosphere in graphite crucibles. Samarium was introduced as SmF_3 with a nominal concentration of 1% or less with respect to Sr or Ba. Luminescence spectra were obtained using a Bruker IFS/66 Fourier Transform spectrometer using a 405 nm diode laser as excitation source. The sample was cooled down to 10 K using a closed cycle cryostat (Oxford Instruments CCC1204). High pressures were achieved using a diamond anvil cell (MiniDAC of D'Anvils Ltd.). The sample chamber consisted of a hole with a diameter of 250 μm drilled into a preindented metal gasket. A single crystal of MFX:Sm^{2+} was placed in the sample chamber along with a crystal of ruby used to calibrate the pressure inside the DAC [20]. Silicone oil was used as the pressure-transmitting medium.

3. Result and discussion

3.1. Emission spectra of BaFBr:Sm^{2+} and SrFBr:Sm^{2+}

Fig. 1 shows the emission spectra of Sm^{2+} in BaFBr and SrFBr host at 10 K under 405 nm excitation. The figure clearly shows the emission bands arising from $^5D_{J(J=0,1,2)} \rightarrow {}^7F_{J(J=1-5)}$ transitions. The low temperature emission spectra enable us to determine the position of the crystal field levels. The energy levels determined from these spectra for both SrFBr:Sm^{2+} and BaFBr:Sm^{2+} are summarized in Table 1. The symmetry assignments in this table are based on the parameterized crystal field parameters (see below) and by comparison with the previously reported spectra for Sm^{2+}-doped SrFCl and BaFCl [16,17,21,22].

3.2. Determination of the free ion and crystal field parameters

The experimental energy levels (Table 1) were used to extract free ion and crystal field parameters. The atomic program developed by the Edvardson and Åberg [23] allows to calculate the energy levels of the lanthanides and actinides for an equivalent electronic configuration using the total Hamiltonian:

$$H = \sum_{k=2,4,6} F^k \hat{f}_k + \sum_i \zeta(r_i)\hat{l}_i \times \hat{s}_i + \alpha\hat{L}^2 + \beta\hat{G}(G_2) + \gamma\hat{G}(R_7) + \sum_{i=2,3,4,6,7,8} T^i \hat{t}_i + \mu_B \vec{B} \times \sum_i \hat{l}_i + 2\hat{S}_i + H_{CF} \quad (1)$$

F^k and ζ are the electronic repulsion and spin–orbit coupling parameters. The f_k are the angular parts of the electronic repulsion. α, β, γ are the Trees parameters associated with the correction for the interaction of two-body configuration. The $\hat{G}(G_2)$ and $\hat{G}(R_7)$ are the Casimir operators for the groups G_2 and R_7. The other configuration interactions include three-body interactions with the operator $\hat{t}_i$ and the associated parameter T^i. The $(\mu_B \vec{B} \times \sum \hat{l}_i + 2\hat{S}_i)$ term describes the standard magnetic field and H_{CF} represents the crystal field Hamiltonian.

This program was included into a routine developed by D. Lovy of our department which uses experimental energy levels and a set of initial parameters of the Hamiltonian as input and subsequently minimizes the differences between calculated and observed energies by changing the values of the selected parameters.

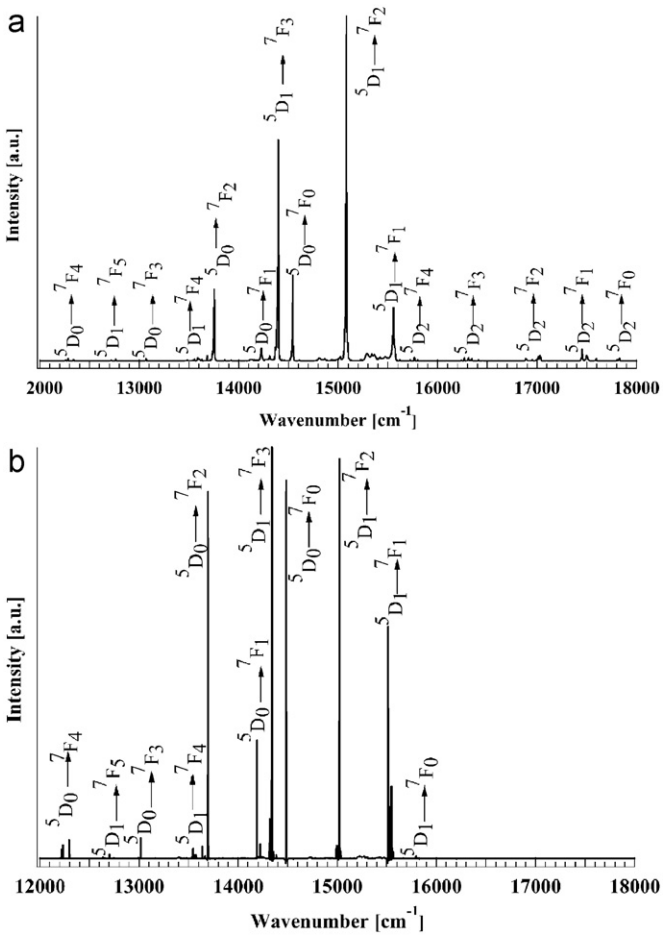

Fig. 1. Luminescence spectra of Sm^{2+} in BaFBr (a) and SrFBr (b) at 10 K at ambient pressure, excited at 405 nm.

In the case of Sm^{2+}, only $^5D_{J(J=0-2)}$ and $^7F_{J(J=0-5)}$ levels are observed. For this reason, only two free ion parameters (F_2 and ζ) were refined, F_4 and F_6 being related to F_2 by $F_4/F_2=0.148$ and $F_6/F_2=0.016$ within the approximation of hydrogen-like wavefunctions [24]. For the refinement of the free ion (F_k and ζ) we have considered the barycenters of ^7F_J and ^5D_J levels as an average of the energy levels, obtained from luminescence spectra (Table 1). The values of α, β, γ, T and B were set to zero. The initial values for the Slater and spin–orbit coupling parameters were taken from the result obtained by Shen et al. [16,17] for BaFCl:Sm^{2+} and SrFCl:Sm^{2+}. The refinement terminates with an average standard deviation of less than five wavenumbers from the observed barycenter values.

The crystal field Hamiltonian for the C_{4v} symmetry as in the MFX system can be written within the one—electron approximation [25],

$$H_{CF} = B_0^2 C_0^2 + B_0^4 C_0^4 + B_4^4\left(C_4^4 + C_{-4}^4\right) + B_0^6 C_0^6 + B_4^6\left(C_4^6 + C_{-4}^6\right) \quad (2)$$

The B_q^k represents the radial parameters of crystal field factors and C_q^k are the angular factors.

The final step is to refine the B_q^k using the previously obtained free ion parameters by taking into account all the observed crystal field energy levels as input. The final overall average difference between the observed and calculated energy levels is less than

Table 1
The crystal field energy levels (relative to $^7F_0$) of Sm^{2+} in BaFBr and SrFBr at 10 K at ambient pressure, determined from Fig. 1. The notation B_x used in table is either B_1 or B_2.

Multiplets	Energy levels (cm^{-1}) BaFBr:Sm^{2+}	Energy levels (cm^{-1}) SrFBr:Sm^{2+}
$^7F_0$	0(A_1)	0(A_1)
$^7F_1$	232.7(A_2)	263.5(A_2)
	317.2(E)	297.5(E)
$^7F_2$	783.3(E)	788.9(E)
	798.6(A_1)	809(B_x)
	811.3(B_x)	818.4(A_1)
	853.7(B_x)	836.9(B_x)
$^7F_3$	1475.6(E)	1470(E)
	1485.5(A_2)	1488.7(A_2)
	1493.2(B_x)	1490.2(E′)
	1504.7(E′)	1493.1(B_x)
	1510.6(B_x)	1511.2(B_x)
$^7F_4$	2205.8(A_1)	2188.3(A_1)
	2238.2(E)	2253.3(E)
	2260.1(A_1)	2257.3(A_2)
	2283.8(E′)	2268.3(E′)
	2289.9(B_x)	2282(A_1)
	2323.0(B_x)	
	2332.9(A_2)	
$^7F_5$	3047.0(E)	
	3089.7(E′)	
	3125.1(A_1)	
	3155.7(E″)	
	3171.0(A_2)	
$^5D_0$	14544.6(A_1)	14485.4(A_1)
$^5D_1$	15878.2(A_2)	15809.0(A_2)
	15887.9(E)	15823.6(E)
$^5D_2$	17770.0(B_x)	
	17803.5(A_1)	17759.1(A_1)
	17821.3(E)	
	17828.4(B_x)	

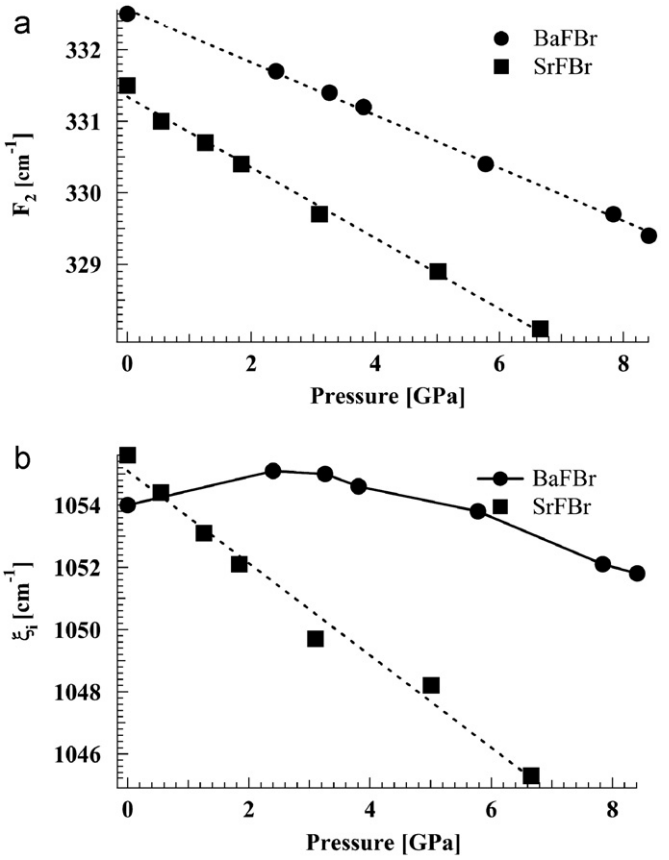

Fig. 2. Free ion parameters under pressure, (a) variation of Slater parameter F_2 (b) variation of ζ.

Table 2
Free ion and crystal field parameters (in cm^{-1}) at ambient pressure of Sm^{2+} in MFX hosts in cm^{-1} units. The values for BaFCl and SrFCl host were taken from Ref. [16,17].

Parameters	BaFCl:Sm^{2+}	BaFBr:Sm^{2+}	SrFCl:Sm^{2+}	SrFBr:Sm^{2+}
F_2	332	332	330.7	331.5
ζ	1058	1054	1057	1055.6
B_0^2	−96	−266	60	−120
B_0^4	−174	−129	−220	−220
B_4^4	−82	−146	−20	−93
B_0^6	398	433	482	463
B_4^6	−196	−136	−236	−191

five wavenumbers. The same procedure was followed to obtain the free ion and crystal field parameters at high pressures. The results obtained at ambient pressure are given in Table 2 as well as the literature values for BaFCl:Sm^{2+} and SrFCl:Sm^{2+} [16,17].

3.3. Pressure dependence on the free ion parameters

Fig. 2 shows the dependence of the F_2 and ζ parameters as a function of pressure of Sm^{2+} in BaFBr and SrFBr. It is clear from this figure that both the parameters decrease upon increasing pressure. The decrease rate of F_2 is similar in both compounds, but ζ shows a stronger pressure dependence in SrFBr than BaFBr (almost 4 times higher for SrFBr).

When a lanthanide ion is incorporated into a crystal field environment, the values of the free ion parameters tend to decrease from their free ion values. This effect is generally described as the nephelauxetic effect [26]. This reduction of F_k and ζ continues on applying pressure. The reduction of free ion parameters can be described with different models. Two models, based on the expansion of the 4f electron cloud inside the crystal, are commonly used to explain the variations of Slater and spin–orbit coupling parameters: the CFC (central-field covalency) and the SRC model (symmetry restricted covalency) [27–29]. The CFC model considers that the expansion of the 4f electron cloud is caused by a spherically symmetric penetration of ligand electrons into the extra valence 4f orbitals. This causes a change in the effective charge Z^* [27].

For the lanthanides, $F_k \propto Z^*$ and $\zeta \propto Z^{*3}$ [28]. Within the approximation of a small reduction of Z^*, the variations are given by Eq. (3),

$$\frac{\Delta F_k}{F_k} = \frac{\Delta Z^*}{Z^*} \quad \text{and} \quad \frac{\Delta \zeta}{\zeta} = 3\frac{\Delta Z^*}{Z^*} \tag{3}$$

Thus, the CFC model predicts that the variation of the spin–orbit coupling parameter is three times more sensitive to pressure than the Slater parameter.

The SRC model [29] considers the participation of 4f orbitals in the formation of molecular orbitals by modifying the symmetry dependent covalency admixture with ligands orbitals. The formation of those orbitals is not spherical but unidirectional and depends on the symmetry of the lanthanide site and position of the ligands. When the covalency is weak, in a good approximation for the modified 4f orbitals, F_k and ζ can be written $F_k \propto N^4$ and $\zeta \propto N^2$, where N represents the renormalization coefficient in terms of a sum including overlap integrals and covalency

parameters. For a small change in F_k and ζ we can write:

$$\frac{\Delta F_k}{F_k} = 4\frac{\Delta N}{N} \quad \text{and} \quad \frac{\Delta \zeta}{\zeta} = 2\frac{\Delta N}{N} \tag{4}$$

From the SRC model we can see that the variation of Slater parameters with pressure should be two times stronger than the variation of the spin–orbit coupling parameter. One useful relation to differentiate these two models is the covalency ratio (*CR*):

$$CR = \frac{\Delta F_2}{F_2} / \frac{\Delta \zeta}{\zeta} \tag{5}$$

From Eq. (5) it is clear that if only the CFC model is responsible for the reduction of free ion parameters, the ratio should be close to 1/3 and for the SRC the corresponding value is 2. The intermediate values indicate the contribution of both models. Combinations of these two models give the form:

$$\frac{\Delta F_k}{F_k} = \frac{\Delta Z^*}{Z^*} + 4\frac{\Delta N}{N} \quad \text{and} \quad \frac{\Delta \zeta}{\zeta} = 3\frac{\Delta Z^*}{Z^*} + 2\frac{\Delta N}{N} \tag{6}$$

The relative changes of F_2 and ζ are calculated from the slopes of Fig. 2 and the changes of effective nuclear charge and renormalization factor are estimated by using Eq. (6). All these values are collected in Table 3.

Shen et al. [17] found that the *CR* is close to 0.5 for Eu^{3+} in LaOBr and LaOCl, which corresponds to the CFC predicted value. The Eu^{3+} replaces the larger La^{3+} ion in LaOCl and LaOBr. In these crystals the 4f orbital of Eu^{3+} is spatially less extended relative to the ligands. The Eu^{3+} ion would experience weak directional interaction with the ligands as predicted by the CFC model. On the other hand Sm^{2+} in MFCl [17], Pr^{3+} in LaOCl [30] and Nd^{3+} in $LaCl_3$ [31] were better described by the SRC model. The lanthanide ions in these crystals have more extended 4f orbitals which lead to directional overlap with the ligands.

Within the pressure range indicated in Table 3, the relative reduction of $\Delta F_2/F_2$ with respect to $\Delta\zeta/\zeta$ is almost 4 times stronger in BaFBr and thus the $CR = 4.43$. This reflects the fact that neither CFC nor SRC alone can explain the *CR*. The SRC model contributes more to the reduction of free ion parameters: the ratio $\Delta N/N$ is three times larger than the ratio $\Delta Z^*/Z^*$ (Table 3). Similar observations were reported for the MFCl:Sm^{2+} system [17]. The higher value of *CR* can be associated with a more expanded 4f wave function of Sm^{2+} in BaFBr host. The effective charge increased upon increasing pressure. The sign reversal of $\Delta Z^*/Z^*$ was observed for Pr^{3+}:GdOCl when $CR > 2$ and increased beyond the value 2 over 5 GPa [30]. The positive value of $\Delta Z^*/Z^*$ can be explained as an increased covalency between the inner shell electrons and the ligands which leads to charge transfer from inner shell to the ligands. This increases the effective nuclear charge Z^* for the 4f electrons. Bungenstock et al. called this effect as "antiscreening" [30]. This behavior is observed for MFCl:Sm^{2+} and for BaFBr:Sm^{2+}.

Table 3
The relative decrease of the F_2 and ζ under pressure for MFBr:Sm^{2+}, together with the relative change of renormalization factor *N* and effective nuclear charge Z^*. The values for MFCl:Sm^{2+} were taken from Ref. [17].

Pressure (GPa)	BaFBr:Sm^{2+}	SrFBr:Sm^{2+}	MFCl:Sm^{2+}
	0–8.4	0–6.7	0–8
$\Delta F_2/F_2$(%)	−0.93	−1.03	−1.17
$\Delta\zeta/\zeta$(%)	−0.21	−0.98	−0.39
$CR = \frac{\Delta F_2}{F_2} / \frac{\Delta\zeta}{\zeta}$	4.43	1.04	3.0
$\Delta N/N$(%)	−0.26	−0.21	−0.31
$\Delta Z^*/Z^*$(%)	0.10	−0.19	0.08

The big difference is the change of ζ with pressure for Sm^{2+} in SrFBr, resulting in a very different *CR* compared to other MFX hosts. For SrFBr:Sm^{2+}, $\Delta N/N$ and $\Delta Z^*/Z^*$ contribute equally to the decrease of F_2 and ζ. This corresponds to a value of *CR* close to one. The CFC model becomes important to describe the reduction of the free ion parameters of SrFBr:Sm^{2+}, as the relative reductions of $\Delta F_2/F_2$ and $\Delta\zeta/\zeta$ are almost equal. One possible explanation for this different behavior of SrFBr:Sm^{2+} system can be related to the lattice parameters of the host crystal. The lattice parameters 'c' and 'a' for matlockite crystals decrease with pressure as well as the '*c*/*a*' ratio. The reduction of the '*c*/*a*' ratio is much higher in SrFBr, compared to the other MFX hosts [32,33]. A similar behavior was observed in the case of Eu^{3+} doped in LaOBr and LaOCl [17].

3.4. Pressure dependence on the crystal field parameters

The variation of crystal field parameters, B_q^k under pressure are shown in Fig. 3. The value of B_0^2 evolves with the same rate for both compounds upon increasing pressure. The sign and magnitude of B_0^2 determine, respectively, the position and splitting of A_2 and E sublevels of $^7F_1$ in the MFX:Sm^{2+} crystals. The B_0^2 changes the sign from negative to positive for SrFBr:Sm^{2+} at 5.5 GPa where we observe the crossing of the two $^7F_1$ sublevels (A_2 and E). This is shown in Fig. 4. For positive values of B_0^2, the A_2 sublevel is higher in energy, as is found in the case of SrFCl:Sm^{2+} [16] at ambient pressure. For negative values of B_0^2, the E sublevel is higher in energy. This is observed in other MFX hosts, like BaFCl [16], SrFBr, BaFBr. The crossing of the two $^7F_1$ sublevels was previously observed in BaFCl:Sm^{2+} at 4 GPa [16].

The other B_q^k parameters show different behavior under pressure for the two compounds (Fig. 3). In particular, the B_0^6 parameter for SrFBr:Sm^{2+} decreases with pressure, in contrast to the increase seen for BaFBr:Sm^{2+}.

A useful parameter to describe the variation of crystal field parameters under pressure is the average crystal field strength *S* [34], which can be expressed as:

$$S = \left\{ \frac{1}{3} \sum_k \frac{1}{2k+1} \left[\left(B_0^k\right)^2 + 2\sum_{q>0} \left|B_q^k\right|^2 \right] \right\}^{\frac{1}{2}} \tag{7}$$

The variation of *S* with unit cell volume is shown in Fig. 5 for SrFBr:Sm^{2+} and BaFBr:Sm^{2+} and compared with the corresponding values for BaFCl:Sm^{2+}, SrFCl:Sm^{2+}, CaFCl:Sm^{2+} obtained by Shen et al. [16,35]. The unit cell volume decreases with increase of pressure for the MFX host compounds [32]. Thus, one can replace pressure by unit cell volume. Fig. 5 shows that going from BaFCl to SrFCl to CaFCl and from BaFBr to SrFBr, the chemical pressure increases due to the smaller size of Ca, Sr compared to Ba. Both physical and chemical pressure show similar variation for the chloride compounds, i.e., *S* increases with pressure. On the other hand for the bromide compounds, chemical pressure leads to a similar variation as for the chloride compounds, but physical pressure results in a different trend. For BaFBr:Sm^{2+}, *S* showed overall increase while the opposite behavior was found for SrFBr:Sm^{2+}. With increasing pressure, the interatomic distances between ligands and the f element decrease. This leads to more interaction between ligand orbitals and the f orbital of the central atom. Thus the average crystal field strength should increase with increase of pressure, as is indeed seen for the BaFCl, SrFCl, CaFCl and BaFBr:Sm^{2+} compounds.

To describe the opposite effect of *S* in SrFBr:Sm^{2+}, we need to take into account the nature of the crystal field parameters.

In MFX crystals, the total CF may be described as a superposition of tetragonal and cubic contributions. The B_0^2 parameter belongs only to the tetragonal component. With increasing

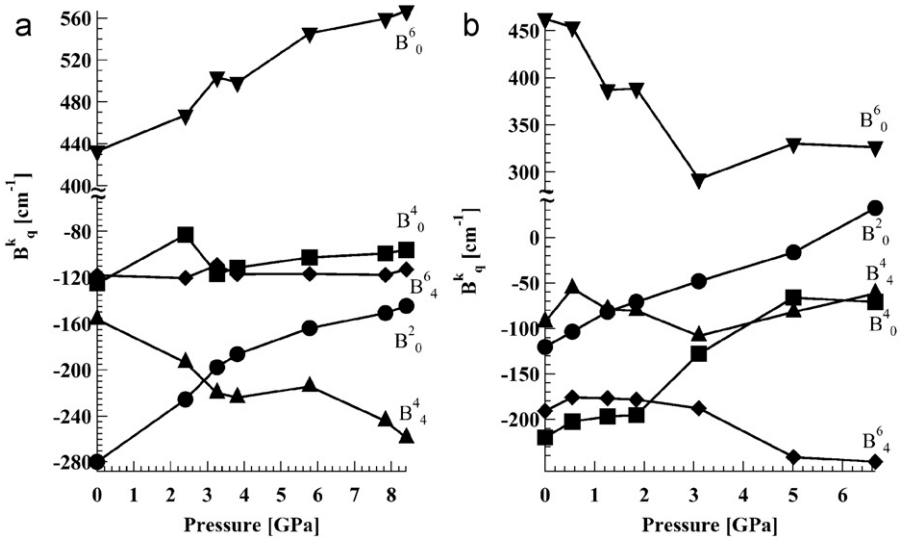

Fig. 3. Variation of crystal field parameters B^k_q under pressure for BaFBr:Sm^{2+} (a) and SrFBr:Sm^{2+} (b).

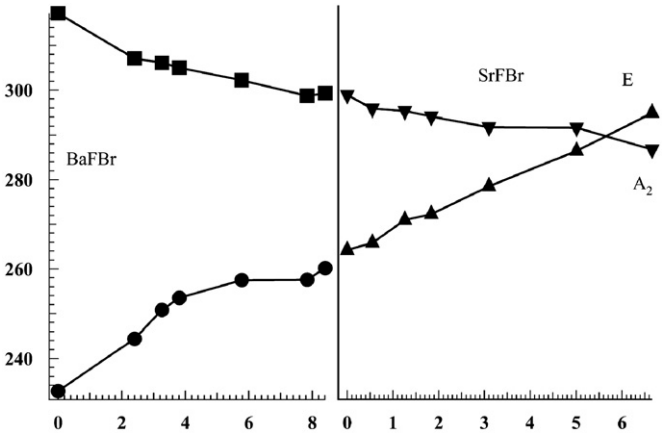

Fig. 4. Variation of the $A_2(^7F_1)$ and $E(^7F_1)$ energy levels under pressure for SrFBr:Sm^{2+} and BaFBr:Sm^{2+}.

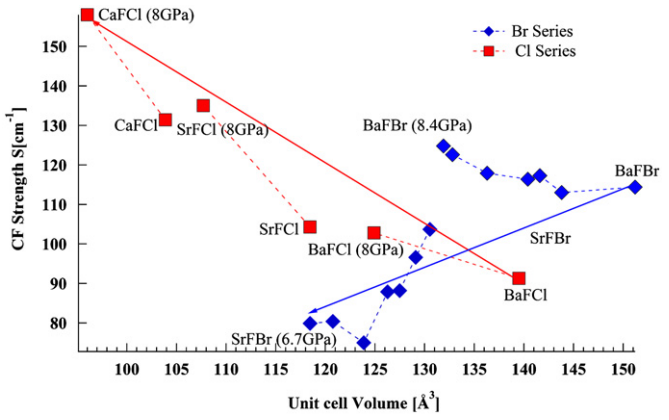

Fig. 5. Variation of average crystal field strength *S*, with unit cell volume of the host crystals.

pressure the absolute value of B^2_0 decreases, indicating a reduction of the tetragonal contribution to the global crystal field. The local compression of the four fluoride and four non axial halide ligands closes the coordination shell of Sm^{2+} and partially screens the influence of fifth, axial halide so that the local coordination approaches regular cubic symmetry. This describes the decrease

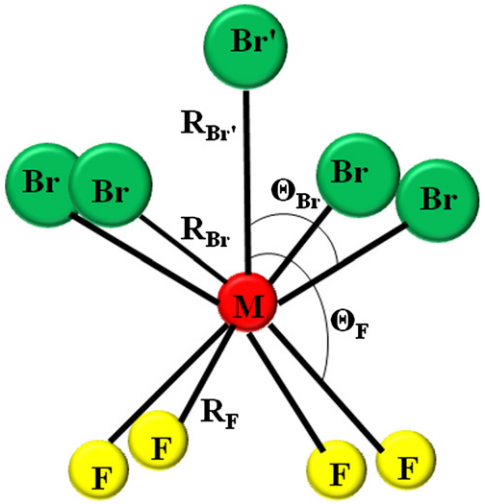

Fig. 6. Coordination polyhedron of F and Br ligands around the central metal atom M in MFBr.

of the average crystal field strength with increasing pressure. A similar trend was observed for Eu^{3+} in lanthanide oxyhalide hosts [36–38].

3.5. Superposition model

The superposition model (SM) [1] assumes that the crystal field created by the ligands surrounding a metal ion in a first coordination sphere is a sum of contributions from the individual ligands. The crystal field parameters can be written as

$$B^k_q = \sum_L \overline{B}_k(R_L) K_{kq}(\Theta_L, \Phi_L)$$

The sum is over the ligands at a position (R_L, Θ_L, Φ_L) and the coordination factors $K_{kq}(\Theta_L, \Phi_L)$ are only functions of the ligands angular directions.$\overline{B}_k(R_L)$ are the intrinsic crystal field parameters and depend only on the kind of ligand (L) at a distance R_L.

The cation coordination polyhedron is shown in Fig. 6. The central metal ion *M* is coordinated with nine anions, four equivalent F anions, four equivalent Br anions and one Br anion marked with Br′ is located on the symmetry axis just above the metal cation. R_F, R_{Br}, $R_{Br'}$ are the distances between the metal

cation and F, Br, Br′ anions, respectively, and Θ_F and Θ_{Br} are the angles between c-axis and anion F and Br, respectively. The corresponding Φ_L are, Φ_F=45°, 135°, 225°, 315° and Φ_{Br}=0°, 90°, 180°, 270°.

The SM allows us to reduce the number of phenomenological crystal field parameters B_q^k to three intrinsic CF parameters $\overline{B}_2$, $\overline{B}_4$and $\overline{B}_6$. Within the frame of SM all the contributions from the ligands can be described by the intrinsic parameters. The intrinsic parameters depend upon the ligand type and the distance between the ligands and the central atom. A convenient way of expressing the distance dependence of the intrinsic parameters is to assume a power low dependence:

$$\overline{B}_k(R) = \overline{B}_k(R_0)\left(\frac{R_0}{R}\right)^{t_k} \tag{8}$$

where R_0 is some arbitrarily chosen standard ligand distance.

We apply the SM to our system (Sm^{2+}:MFBr; M=Ba, Sr) to understand the CF created by the surrounding ligands. The B_0^k and B_4^k (k=4, 6) can be expressed by using Eqs. 7) and (8) as

$$B_0^k = \overline{B}_k(R_{Br})\overline{K}_{k0}^{Br} + \overline{B}_k(R_F)K_{k0}^F,\ B_4^k = \overline{B}_k(R_{Br})K_{k4}^{Br} + \overline{B}_k(R_F)K_{k4}^F \tag{9}$$

where

$$\overline{K}_{k0}^{Br} = K_{k0}^{Br} + \left(\frac{R_{Br}}{R_{Br'}}\right)^{t_k^{Br}} \tag{10}$$

In Eq. 9) K_{kq}^{Br} and K_{kq}^F are the collective coordination factors for 4 Br and 4 F equidistant ligands at a distance R_{Br} and R_F, respectively. Eq. (10) includes the fact that the four equivalent Br ions at the distance R_{Br} contributes to the term K_{k0}^{Br} and the axial Br′ ion at distance $R_{Br'}$ with different strength $\overline{B}_k(R_{Br'}) = \overline{B}_k(R_{Br})(R_{Br}/R_{Br'})^{t_k^{Br}}$. These coordination factors can be calculated at each pressure knowing the value of Θ_{Br} and Θ_F using the following relations [39],

$$K_{40}^L = \frac{1}{2}(35\cos^4\Theta_L - 30\cos^2\Theta_L + 3)$$

$$K_{44}^L = \pm\frac{35}{2\sqrt{70}}\sin^4\Theta_L$$

$$K_{60}^L = \frac{1}{4}(231\cos^6\Theta_L - 315\cos^4\Theta_L + 105\cos^2\Theta_L - 5)$$

$$K_{64}^L = \pm\frac{63}{12\sqrt{14}}(11\cos^2\Theta_L - 1)\sin^4\Theta_L$$

where for the K_{k4}^L collective coordination factors the "+" sign refers to the value for Br ions and "−" for the F ions, due to the different value $\cos^4\Phi_F = -1$.

The structural parameters at each pressure were determined by the DFT calculations (see appendix). $\overline{B}_k(R_{Br})$ and $\overline{B}_k(R_F)$ were determined using the two linear equations Eq. (9) at each pressure from the B_0^k and B_4^k (Fig. 3). As the ionic radius of Sm^{2+} is smaller than Ba^{2+}, one has to take account local distortion around Sm^{2+} ions in BaFBr. We use two sets of distortion values (distortion 1: ΔR_{Br} = −7 pm, ΔR_F = −6 pm, $\Delta\Theta_{Br}$ = −1°, $\Delta\Theta_F$ = −1° and distortion 2: ΔR_{Br} = −9 pm, ΔR_F = −8 pm, $\Delta\Theta_{Br}$ = −1.5°, $\Delta\Theta_F$ = −1.5°) for the determination of intrinsic parameters of BaFBr:Sm^{2+} with same exponent t_k^{Br} value that was determined by Shen et al. [16] for the MFCl:Sm^{2+} system. We assume that the distortion around Sm^{2+} in BaFBr remains unchanged with pressure. The final values of $\overline{B}_k(R_{Br})$ and $\overline{B}_k(R_F)$ were plotted for SrFBr:Sm^{2+} and BaFBr:Sm^{2+} along with BaFCl:$Sm^{2+}$and SrFCl:Sm^{2+} in Fig. 7 against ligand-metal distance. The $\overline{B}_k(R_{Cl})$ and $\overline{B}_k(R_F)$ for BaFCl:Sm^{2+} and SrFCl:Sm^{2+} were taken from the study of Shen et al. [16].

The $\overline{B}_4(R_{Br})$ and $\overline{B}_6(R_{Br})$ in BaFBr:Sm^{2+} (Fig. 7) show the same trend with BaFCl:Sm^{2+} and SrFCl:Sm^{2+}. Using higher distortion (distortion 2) does not affect these two intrinsic parameters. Only

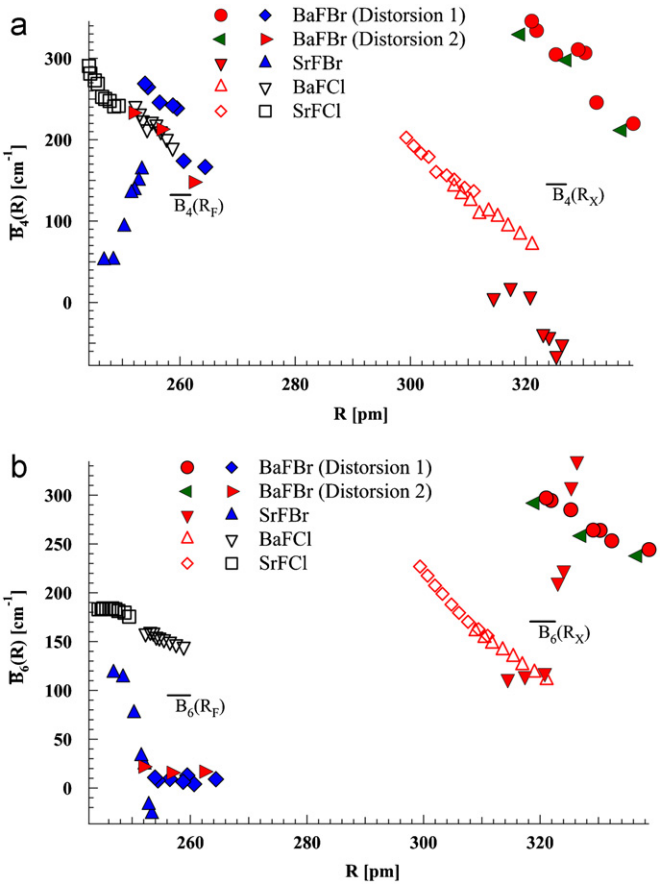

Fig. 7. Intrinsic $\overline{B}_4(R_L)$ (a) and $\overline{B}_6(R_L)$ (b) crystal field parameters as a function of metal-ligand distance.

$\overline{B}_4(R_F)$ changes in such a way it follows the same line of the MFCl system.

Distinct differences are noticed in the case of $\overline{B}_6(R_F)$ in Fig. 7(b) for the two above mentioned compounds. $\overline{B}_6(R_F)$ is unusually small for BaFBr:Sm^{2+} compound and it is also unaffected with small change of local distortion. Thus small changes of local distortion around Sm^{2+} ion do not affect the intrinsic parameters if the exponent (t_k^{Br}) value does not vary.

The SM model is unable to explain the behavior of crystal field strength of SrFBr:Sm^{2+}. From this model one expects an increase of intrinsic CF with decrease of ligand-metal distance [Eq. (8)]. In Fig. 7 we can see the trend is completely opposite for $\overline{B}_4(R_F)$ and $\overline{B}_6(R_{Br})$.

At ambient pressure the collective coordination factors in Eq. (9) show partial cancellation: K_{44}^{Br} = 1.5551, K_{44}^F = −1.1145, K_{64}^{Br} = 0.5376, K_{64}^F = −1.4732 for BaFBr:Sm^{2+}. Due to the opposite signs of the factor pairs (K_{44}^{Br},K_{44}^F) and (K_{64}^{Br}, K_{64}^F), there can be a strong cancellation between the contributions of the Br and F ligands, which results in the smaller value of $\overline{B}_6(R_F)$. One can find from Fig. 7 the ratio $\overline{B}_6/\overline{B}_4 = 0.05$ for the F ligands and $\overline{B}_6/\overline{B}_4 = 1.11$ for the Br ligands at ambient pressure for BaFBr:Sm^{2+}. This suggests that the contribution of $\overline{B}_6(R_F)$ is very small compared to the one of the Br ligands.

One of the limitations of the SM model is the neglect of ligand–ligand interactions, as was demonstrated by Curtis and Newman for $PrCl_3$ [40]. They showed that for $PrCl_3$ these interactions contributed about 15% to the $\overline{B}_6$ parameters. Ab initio calculations on crystal field parameters of Sm^{2+} in BaFCl and SrFCl [41] showed that the calculated values of the intrinsic crystal field parameters of the chlorides were lower than the experimental ones, while the opposite was found for the intrinsic parameters of the fluorides. This behavior suggested [41] the presence of

fluoride–chloride interactions which transfer partially crystal field contributions from one ion to the other.

The breakdown of SM for SrFBr:Sm^{2+} can be interpreted by taking into account the high decrease rate of the 'c/a' ratio with pressure compared to the other matlockite hosts [32,33]. This leads to increase ligand-ligand interactions not only within F ligands but also between Br ligands. It was found previously for Sm^{2+} doped in mixed $SrFCl_xBr_{1-x}$ ($0 \le x \le 1$) crystals that the ligands in the second coordination sphere play an important role in the crystal field [14]. This also suggests that the ligand-ligand and metal-metal interactions within the neighboring coordination spheres are not negligible. Ab initio calculation of crystal field of Sm^{2+} in SrFBr including the above mentioned interactions could be helpful to understand this behavior.

4. Conclusion

The free ion and crystal field parameters were determined from emission spectra of Sm^{2+} in BaFBr and SrFBr host at ambient pressure and at high pressures.

We have demonstrated that with increasing pressure the free ion parameters decrease from ambient pressure value. The nephelauxetic effect was described by both CFC and SRC models. The CFC model was more applicable to SrFBr:Sm^{2+} system while SRC models explains better the variation for BaFBr:Sm^{2+} system.

The crystal field parameters showed different trend with pressure. Only B_0^2 was found to present a similar trend for both the compounds. The average crystal field strength shows different behavior for both compounds. The SM is unable to explain the unusual behavior of the intrinsic crystal field parameters of the Sm^{2+} ion in the SrFBr host. Ligand–ligand interactions are probably at the origin of this behavior.

Acknowledgments

This work was supported by the Swiss National Science Foundation. We thank D. Lovy for implementing and developing the program for the crystal field calculation.

Appendix A. Structural parameters optimization of BaFBr and SrFBr systems

All the systems were treated with density functional theory (DFT) calculation [42,43], performed within the general gradient approximation (GGA) [44,45] to the exchange correlation energy. The GGA showed better agreement with experiment for pressure dependent structural and vibrational properties of BaFCl [46]. The calculations were performed using ABINIT [47–49] package which is based on pseudopotentials and plane waves. For all the ions optimized (RRKJ) pseudo potentials [50] in the separable Kleinman–Bylander form [51] were used. The pseudo potentials were generated by using the OPIUM [52] program, taking for the Ba atom scalar relativistic effects [53] into account. A $10 \times 10 \times 5$ k-point Monkhorst–Pack grid [54] was employed and the wave-functions were expanded in plane-waves up to a kinetic energy cut-off of 40 Hartree.

During the optimizations, the symmetry of the systems was kept fixed to the tetragonal space group P4/nmm (no. 129): Ba^{2+} and Sr^{2+} are on a site 2c (1/4, 1/4, z_M), (M=Ba, Sr); Br^- is on a site 2c positions (1/4, 1/4, z_{Br}); and F^- is on a 2a site (3/4, 1/4, 0). The phonon calculations [55] confirmed that all the structures are minima of the potential energy surface, since there are no negative frequencies.

See below for Table A1

Table A1
Experimental (taken from Refs. [56,57]) and calculated (this work) (GGA) structural parameters for BaFBr and SrFBr at ambient pressure.

	BaFBr (this work)	BaFBr (ref. [56])	SrFBr (this work)	SrFBr (ref. [57])
a (Å)	4.570	4.508	4.244	4.218
c (Å)	7.626	7.441	7.687	7.337
z_{Br}	0.6496	0.6472	0.6535	0.6479
z_M	0.1895	0.1911	0.1799	0.1859

References

[1] D.J. Newman, Betty Ng, Rep. Prog. Phys. 52 (1989) 699.
[2] C.K. Jayasankar, F.S. Richardson, M.F. Reid, J. Less-Common Met. 148 (1989) 289.
[3] J. Rubio O., J. Phys. Chem. Solids 52 (1991) 101.
[4] R. Jaaniso, H. Bill, Europhys. Lett. 16 (1991) 569.
[5] Y.R. Shen, T. Gregorian, W. Holzapfel, High Pressure Res. 7 (1991) 73.
[6] Z. Liu, T. Massil, H. Riesen, Physics Procedia 3 (2010) 1539.
[7] Z. Liu, M. Stevens-Kalceff, H. Riesen, J. Phys. Chem. C 116 (2012) 8322.
[8] H. Riesen, W.A. Kaczmarek, Inorg. Chem. 46 (2007) 7235.
[9] S. Sakirzanovas, A. Katelnikovas, D. Dutczak, A. Kareiva, T. Jüstel, J. Lumin. 131 (2011) 2255.
[10] M.-C. Wiegand, W. Sievers, J.K.N. Lindner, Th. Tröster, S. Schweizer, J. Lumin. 131 (2011) 2400.
[11] A. Ohnishi, K. Kan'no, Phys. Status Solidi B 245 (2008) 2815.
[12] K. Takahashi, J. Lumin. 100 (2002) 307.
[13] H. Hagemann, P. Tissot, D. Lovy, F. Kubel, H. Bill, J. Therm. Anal. Calorim. 57 (1999) 193.
[14] R. Jaaniso, H. Hagemann, H. Bill, J. Chem. Phys. 101 (1994) 10323.
[15] D. Nicollin, H. Bill, J. Phys. C: Solid State Phys. 11 (1978) 4803.
[16] Y.R. Shen, W.B. Holzapfel, Phys. Rev. B 51 (1995) 15752.
[17] Y.R. Shen, W.B. Holzapfel, Phys. Rev. B 52 (1995) 12618.
[18] P. Pal, H. Hagemann, Proceedings of the Seventh International Conference on F Elements, Terrae Rarae, Gerd Meyer eds., 06 (2009) p1.
[19] T. Penhouet, H. Hagemann, J. Alloys Compd. 451 (2008) 74.
[20] K. Nakano, Y. Akahama, Y. Ohishi, H. Kawamura, Jpn. J. Appl. Phys. 39 (2000) 1249.
[21] G. Grenet, M. Kibler, A. Gros, J.C. Souillat, J.C. Gacon, Phys. Rev. B 22 (1980) 5052.
[22] J.C. Gacon, G. Grenet, J.C. Souillat, M. Kibler, J. Chem. Phys. 69 (1978) 868.
[23] S. Edvardsson, D. Åberg, Comput. Phys. Commun. 133 (2001) 396.
[24] G.H. Dieke, Spectra and Energy Levels of Rare Earth Ions in Crystals, Interscience Publishers, Wiley, 1968.
[25] B.G. Wybourne, Spectroscopic Properties of Rare Earths, Wiley, New York, 1965.
[26] C.K. Jorgensen, R. Reisfeld, Inorg. Chem. Concepts 1 (1977), Lasers and Excited States of Rare Earths.
[27] Q. Wang, A. Bulou, J. Phys. Condens. Matter 5 (1993) 7657.
[28] R. D. Cowan, Theory At. Struct. Spectra, 1981.
[29] D.J. Newman, B. Ng, Y.M. Poon, J. Phys. C 17 (1984) 5577.
[30] C. Bungenstock, Th. Tröster, W.B. Holzapfel, Phys. Rev. B 62 (2000) 7945.
[31] Th. Tröster, T. Gregorian, W.B. Holzapfel, Phys. Rev. B 48 (1993) 2960.
[32] F. Decremps, M. Fischer, A. Polian, J.P. Itié, M. Sieskind, Eur. Phys. J. B 9 (1999) 49.
[33] Y.R. Shen, U. Englisch, L. Chudinovskikh, F. Porsch, R. Haberkorn, H.P. Beck, W.B. Holzapfel, J. Phys. Condens. Matter 6 (1994) 3197.
[34] N.C. Chang, J.B. Gruber, R.P. Leavitt, C.A. Morrison, J. Chem. Phys. 76 (1982) 3877.
[35] Y.R. Shen, W.B. Holzapfel, J. Phys. Condens. Matter 7 (1995) 6241.
[36] Q. Wang, A. Bulou, Solid State Commun. 94 (1995) 309.
[37] Y. Chi, S. Liu, W. Shen, L Wang, G. Zou, Physica B+C 139-140 (1986) 555.
[38] Y. Chi, S. Liu, H. Li, X. Zhao, L. Wang, J. Alloys Compd. 256 (1997) 1.
[39] D.J. Newman, Betty Ng, Crystal Field Handbook, Cambridge University Press, 2000.
[40] M.M. Curtis, D.J. Newman, J. Chem. Phys. 52 (1970) 1340.
[41] Y. Shen, K.L. Bray, Phys. Rev. B 58 (1998) 5305.
[42] P. Hohenberg, W. Kohn, Phys. Rev. 136 (1964) B864.
[43] W. Kohn, L.J. Sham, Phys. Rev. 140 (1965) A1133.
[44] J.P. Perdew, K. Burke, M. Ernzerhof, Phys. Rev. Lett. 77 (1996) 3865.
[45] J.P. Perdew, K. Burke, M. Ernzerhof, Phys. Rev. Lett. 78 (1997) 1396.
[46] V. D'Anna, L.M. Lawson Daku, H. Hagemann, F. Kubel, Phys. Rev. B 82 (2010) 024108.
[47] X. Gonze, et al., Comput. Mater. Sci. 25 (2002) 478.
[48] X. Gonze, et al., Z. Kristallogr. 220 (2005) 558.
[49] ABINIT code, a common project of the Université Catholique de Louvain, Corning Incorporated, the Université de Liège, the Commissariat á l'Energie Atomique, Mitsubishi Chemical Corp., the Ecole Polytechnique Palaiseau, and other contributors (URL 〈http://www.abinit.org〉).
[50] A.M. Rappe, K.M. Rabe, E. Kaxiras, J.D. Joannopoulos, Phys. Rev. B 41 (1990) 1227.

[51] L. Kleinman, D.M. Bylander, Phys. Rev. Lett. 48 (1982) 1425.
[52] 〈http://opium.sourceforge.net〉 (last visited: 01.02.2012).
[53] I. Grinberg, N.J. Ramer, A.M. Rappe, Phys. Rev. B 62 (2000) 2311.
[54] H.J. Monkhorst, J.D. Pack, Phys. Rev. B 13 (1976) 5188.
[55] X. Gonze, C. Lee, Phys. Rev. B 55 (1997) 10355.
[56] B. Liebich, D. Nicollin, Acta Crystallogr., Sect. B: Struct. Crystallogr. Cryst. Chem. 33 (1977) 2790.
[57] H.P. Beck, J. Solid State Chem. 17 (1976) 275.